IEEE Access
Multidisciplinary | Rapid Review | Open Access Journal

Received July 21, 2020, accepted July 27, 2020, date of publication August 3, 2020, date of current version August 14, 2020.

Digital Object Identifier 10.1109/ACCESS.2020.3013655

A Novel Dissemination Protocol to Deploy Opportunistic Services in Federated Satellite Systems

JOAN A. RUIZ-DE-AZUA[1,2,3], (Member, IEEE), ANNA CALVERAS[1], AND ADRIANO CAMPS[2,3], (Fellow, IEEE)

[1]Department of Network Engineering, Universitat Politècnica de Catalunya (UPC)—BarcelonaTech, 08034 Barcelona, Spain
[2]CommSensLab-UPC María de Maeztu Unit, Department of Signal Theory and Communications, Universitat Politècnica de Catalunya (UPC)—BarcelonaTech, 08034 Barcelona, Spain
[3]Institut d'Estudis Espacials de Catalunya (IEEC), Research Group in Space Science and Technologies of Universitat Politècnica de Catalunya (CTE-UPC), 08034 Barcelona, Spain

Corresponding author: Joan A. Ruiz-de-Azua (joan.adria@tsc.upc.edu)

This work was supported in part by the ''CommSensLab'' Excellence Research Unit Maria de Maeztu Ministerio de asuntos Económicos y transformación digital (MINECO) under Grant MDM-2016-0600; in part by the Spanish Ministerio de Ciencia e Innovación (MICINN) and European Union - European Regional Development Fund (EU ERDF) project ''Sensing with pioneering opportunistic techniques'' under Grant RTI2018-099008-B-C21; in part by the Agència de Gestió d'Ajuts Universitaris i de Recerca (AGAUR)—Generalitat de Catalunya (FEDER) under Grant FI-DGR 2015; and in part by the Secretaria d'Universitats i Recerca del Departament d'Empresa i Coneixement de la Generalitat de Catalunya under Grant 2017 SGR 376 and Grant 2017 SGR 219.

ABSTRACT Earth Observation applications are demanding higher spatial resolution and shorter revisit times than existing systems, which can be met by ad-hoc constellations of Federated Satellite Systems. These systems are distributed satellite architectures which rely on the collaboration between satellites that share unused resources, such as memory storage, computing capabilities, or downlink opportunities. In the same context, the Internet of Satellites paradigm expands the federation concept to a multi-hop scenario, without predefining a particular satellite system architecture, and deploying temporal satellite networks. The basis of both concepts is the offer of unused satellite resources as services. Therefore, it is necessary that satellites notify their availability to the other satellites that compose the system. This work presents a novel Opportunistic Service Availability Dissemination Protocol, which allows a satellite to publish an available service to be consumed by others. Details of the protocol behavior, and packet formats are presented as part of the protocol definition. The protocol has been verified in a realistic scenario composed of Earth Observation satellites, and the Telesat mega-constellation as network backbone. The achieved results demonstrate the benefits of using a protocol as the proposed one, which in some cases even doubles the amount of data that can be downloaded. To the best of our knowledge, this proposal is the first protocol that allows deploying opportunistic services for Federated Satellite Systems.

INDEX TERMS Federated satellite systems, satellite networks, inter satellite network, Internet of Satellites, earth observation.

I. INTRODUCTION

Nowadays, novel space applications have emerged to satisfy current environmental, socio-economic, and geo-political demands. The Horizon 2020 Operational Network of Individual Observation Nodes (ONION) project [1] identified the needs of the Earth Observation (EO) community. Specifically, applications to monitor marine weather forecast, and marine fishery pressure are the most demanded ones to cover Arctic changes, followed by hydric stress monitoring (i.e. soil moisture) as a proxy of desertification, and crop yield, among other effects. Moreover, the increase of climate disasters have accentuated the need of a continuous monitoring and an accurate prediction mechanism [2]. As pointed out in [3], these applications can only be achieved with low latency and sub-metric spatial resolution observations. The consequence

The associate editor coordinating the review of this manuscript and approving it for publication was Mohammad Tariqul Islam.

This work is licensed under a Creative Commons Attribution 4.0 License. For more information, see https://creativecommons.org/licenses/by/4.0/

of having an instrument that provides these measurements would entail the increase of the data volume generated by the satellite.

Some proposals have addressed this challenge by intelligently reducing the generated amount of data by means of data compression [4], or as in the case of the FSSCat mission [5] by discarding useless generated data. Specifically, this mission includes the ϕ-sat-1 technology demonstrator [6], an hyperspectral camera with an Artificial Intelligence (AI) processor that discards images covered by clouds. Even though these optimizations, the problem of downloading the large volumes of useful data generated still remains. Monolithic satellite missions have normally addressed this situation by using more ground stations. Placing these stations in strategic locations increments the number of contacts with the satellite, and thus the capacity to download data. Nevertheless, this approach is limited to transferring data over a set of ground stations, being difficult to achieve a low latency (i.e. near-real-time services). Additionally, the use of a large ground station network considerably raises the mission cost. Despite these difficulties, the improvement of the download capacity still seems the correct strategy.

Distributed Satellite Systems (DSS) have emerged as a moderate-risk and cost-effective solution to meet these new demands. DSS are described as an ensemble of satellites that share a global and common objective. As presented in [7], different DSS architectures have been proposed in the last years. Some of them include satellite-to-satellite communications [8]. In this context, a satellite could download data using the ground station contact of another satellite, increasing thus the overall download capacity. The Federated Satellite System (FSS) concept [9] aims at addressing this situation by promoting collaborations between satellites to share unused resources, such as memory storage or downlink opportunities. These collaborations, called *federations*, are established sporadically and opportunistically depending on the availability of the resources to be shared. The federation is established through an Inter-Satellite Link (ISL), which is a point-to-point communication link between satellites. Due to satellite dynamics, an ISL is characterized by being feasible only during a lapse of time, impacting the federation stability.

To overcome this situation, the Internet of Satellites (IoSat) paradigm [10] expands this concept to a multi-hop scenario, and without predefining any satellite system architecture. In this paradigm, satellites decide to deploy sporadic and temporal networks, called Inter-Satellite Networks (ISN). These networks are composed of satellites that work as intermediate nodes, transferring data from a source to a destination. Note that these networks follow the nature of the federations, being created only when they are needed (i.e. on-demand). This IoSat paradigm introduces new communications challenges due to its opportunistic nature. The challenge of deploying and constructing an ISN has previously been discussed in [11]. Specifically, the definition of the network is characterized by the identification of the different routes composed of satellites that remotely interconnect two of them. The routing protocol is responsible of performing this task in each satellite.

The basis of the FSS and the IoSat paradigms is the possibility to opportunistically share unused satellite resources. These resources are commonly used by the satellite itself, which changes their state over time. A traditional satellite design always ensures the availability of these resources by oversizing them. For this reason, satellites can have excess capacity at certain moments of the mission, being able to offer them as services. Those satellites are known as service *providers*, and the ones that use the services are known as *customers*. Due to the state fluctuation of the resources, the associated service is not always available. This temporal availability generates valuable opportunities to consume the service that should be used by the customers. Therefore, a mechanism to notify the available services must be designed to catch these opportunities.

Previous research [12] centered on fairly assigning the value of the satellite resources according to the provider concurrence, and customer demand. An operational model was developed in [13] to allocate processing, storage and communication resources to computational demands. An optimal solution to process satellite tasks, allocate links, store and delivery data is determined by means of a mixed-integer linear programming (MILP) formulation. A trusted auctioneer leverages on a mechanism to allocate the resources, and suggest prices for exchanging resources across the federation. This centralized approach can compensate the adverse effects of strategic biddings on collective value, and increases the number of resources exchanged in a federation. A similar mechanism to manage and distribute the available services based on pricing and auctions is proposed in [14]. The proposed solution uses the communications protocol stack presented in [15] to exchange information about the auctions status between the satellites. This protocol stack enables the satellites to constantly transmit information about the network status, in addition to the details of the available services. Although this approach is functional, constant transmissions can provoke a waste of power for those satellites that are isolated, and do not participate in the network. Furthermore, all the satellites are transmitting network information while they are not providing any kind of service. Thus, this approach is not suitable for sporadic and opportunistic scenarios, such as IoSat and FSS. A more efficient mechanism must be conceived.

This work proposes the Opportunistic Service Availability Dissemination Protocol (OSADP) to deal with this situation. This protocol performs the publication of the available services following a decentralized transmission. In particular, this publication is done only by the service providers, which is intelligently forwarded node-by-node, and its propagation is bounded. Thanks to this adjustment, unnecessary transmissions from other satellites are avoided. Once a satellite receives this publication and is interested to consume the service, it can establish the federation using the protocol

presented in [16]. Note that the pricing algorithm presented in [14] can also be executed using the OSADP.

This work presents thus the details of the protocol, and its performance after simulating it in a realistic scenario. The protocol is evaluated in a scenario that includes different EO satellites (currently orbiting) that generate data, and download it using the capabilities of the other satellites thanks to the OSADP. Additionally, the Telesat mega-constellation [17] has been included in the scenario as a network backbone to increase the connectivity of the network. The analysis is conducted using the satellite network simulation engine presented in [18]. The results demonstrate the benefits of using the OSADP to notify downlink opportunities among the satellites, highly increasing the amount of downloaded data. Additionally, they demonstrate that a mega-constellation can be really useful also for satellite-to-satellite applications.

In summary, the presented work provides: 1) a detailed description of the OSADP and its features, 2) a performance analysis evaluating the benefits of applying this protocol, 3) a topology study of applying a mega-constellation as a network backbone, and 4) proofs of the benefits of using mega-constellations for satellite-to-satellite applications.

The remainder of the article is structured as follows. First, Section II discusses the nature of the services and presents the details about the OSADP. The simulation scenario and the satellite model are then presented in Section III. Characteristics of the simulation engine are detailed in Section IV. The analysis and results are exposed in Section V. Finally, Section VI concludes the work.

II. OPPORTUNISTIC SERVICE AVAILABILITY DISSEMINATION PROTOCOL

In all missions, the satellite has to perform different actions that are scheduled over time (e.g. payload execution, communications with the ground station), which conform the well-known *mission plan*. Different researchers have been working on conceiving mechanisms to design the optimum plan [19], [20]. All of them have remarked the importance to properly model satellite *resources* [21]. In this context, a resource is an abstract object that encapsulates a system capacity, which is typically associated to a satellite subsystem or device (e.g. the available power is associated to the batteries). However, other less tangible resources have also been considered crucial for the mission. It is the case of the mission plan defined in [22], which also considers ground station contacts as an important satellite resource.

These resources are consumed or released by the different actions that the satellite must perform, known as satellite *tasks*. These tasks change the state of the resources over time. Normally, resources are oversized to always ensure its availability. Therefore, satellites have excess capacity at certain moments of the mission, being able to offer this excess to others. The FSS approach [9] proposes the interaction of satellites to optimize these unused resources. In this regard, a satellite offers its remaining resources as *services*, known as the service *provider*. These services can be consumed by other satellites to perform their tasks, known as *customers*, and can be offered only when they are available. For instance, a satellite can offer the service to download data because it is in contact with a ground station.

Due to the fluctuation of the resources usage, the service is not always available. The corresponding service becomes thus time-dependent, being just available during a lapse of time, known as *service lifetime*. This temporal availability generates valuable opportunities to consume the service by the other satellites. Therefore, a notification of the available services must be designed to catch these temporal opportunities. The proposed OSADP aims at addressing this challenge following a decentralized publish mechanism. With this technique, a satellite provider periodically publishes a service only when it is available.

The dissemination of the publication is crucial to correctly notify the satellites, and at the same time not saturating the network with unnecessary messages. However, the main purpose of this publication is to notify as many satellites as possible. Therefore, an intelligent dissemination to satisfy both requirements has been considered in the OSADP. The proposed mechanism is based on the Originator Messages (OGM) propagation in the Better Approach To Mobile Adhoc Networking (BATMAN) [23] and BatMan eXperimental version 6 (BMX6) [24] protocols. In particular, the propagation of a publication is conducted node-by-node, in which each node or satellite processes the packet accordingly. When a node receives a publication that contains information about the availability of a service, it evaluates if it is interested in consuming this service or not. If it is the case, it replies requesting a federation, following the protocol presented in [16]. Otherwise, it forwards the publication to its neighbors. Note that this propagation not only notifies the neighbors, but it also indicates that the node accepts and commits to be part of a possible route as an intermediate node. If it is not the case, the node does not propagate the publication. Additionally, a received publication from a neighbor is discarded if the node detects that it has already been propagated.

Figure 1 presents an example of this publication process in a network composed of different satellites (S_0, S_1, S_2, S_3, S_4 and S_5), in which the satellite S_0 is the provider, and the

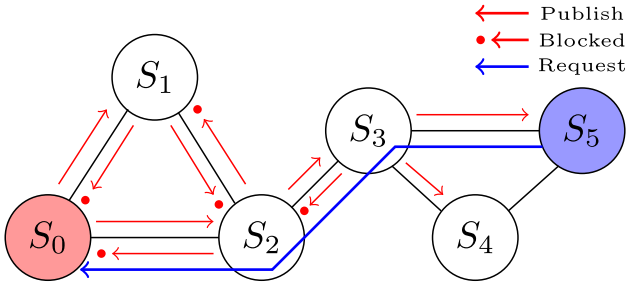

FIGURE 1. Representation of the publication process between the satellite provider (S_0) and the customer (S_5).

satellite S_5 the customer. In this example, the nodes propagate the publication of the provider (red arrows), blocking those that are duplicated (red arrows with a dot). The dissemination process is thus optimized by only propagating useful notifications. Additionally, in this case satellite S_4 does not propagate the publication because it does not commit to be an intermediate node in a possible route due to its limited resources. Finally, the customer requests the service after receiving the publication.

All these intermediate decisions are possible because a `publish` packet is propagated. This packet contains information of the available service structured in different fields. Figure 2 presents this structure composed of 13 bytes, including 11 bits reserved for future extensions. At the very beginning of the structure, the field *type* identifies that the packet is a publication using a single bit, and the following field indicates the available *service* category with four bits (e.g. data downlink). These two fields, restrained in a byte, are accompanied with three bits reserved for the definitions of future services types. The provider of the service is determined with the *provider identifier*, which enables to distinguish multiple services from the same provider or different providers offering the same kind of service. This identifier is represented with three bytes, allowing it to identify more than 16 millions of satellites.

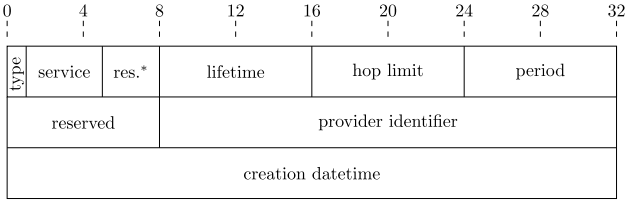

FIGURE 2. Structure of the `publish` packet (bit unit).

A Service Table (ST) is generated in each node to register in different entries the available services from each provider. A new entry is generated when a new publication is received, storing the corresponding provider and the service. This entry shall be removed when the service is no longer available. Therefore, an expiration date is associated with each entry, computed using the estimated *Service Lifetime* (SLT) field of the `publish` structure. Additionally, a service may be not available because the provider is unreachable from the node. Therefore, the corresponding entry is updated with every received publication, periodically transmitted by the provider. Using the *Period* field, a node considers the loss of the provider if no publication is received after three timeouts, then it removes the corresponding entry.

After the entry update, the publication is propagated to the neighbors. As indicated previously, this propagation is performed intelligently, discarding useless publications. In particular, the same `publish` packet can be received from different neighbors. When a node receives a publication of the same provider with the same service, it can detect packet duplicity thanks to the *creation datetime* field. This field corresponds to the timestamp at which the packet has been transmitted by the provider. This time is updated in each periodic transmission. Therefore, if two (or more) received publications have the same date, they are duplicated. Additionally, this parameter enables the detection of old publications that remain in the network. If the received packet has a creation date older than the stored one, it is outdated, and thus discarded.

The propagation of this `publish` packet can be bounded thanks to the *Hop Limit* (HL) field. This parameter has largely been used in the Internet, and it limits the number of hops that a `publish` packet can travel into a network. In the OSADP case, this value corresponds to the hop limit or number of forwards between nodes of the `publish` packet. Therefore, the HL starts with an initial non-negative integer, which is decremented by one before being forwarded by each node. When the HL value becomes zero, the packet is thus discarded. This parameter enables thus to control the diameter of the network in which the publication is disseminated. Note that an additional byte is reserved considering possible extensions of the HL, SLT, and period values.

Figure 3 summarizes the previous decision process in each node for a specific service s_k in a flow diagram. Note that an accurate terminology has been used in the diagram, where S corresponds to the state of the OSADP related to service s_k. This state can be *PUB* for publication state, *PROV* for provider state, and *CUST* for customer state in the federation. Moreover, *pb* corresponds to the `publish` packet of the service current s_k, which is transmitted every T_k period, and at the transmission time t_k^{tx}. The service lifetime STL_k associated to the service s_k enables to compute its expiration date t_k^d. The creation date of *pb* is represented as t_k^c, being ascribed at the current time t. Additionally, a received packet p_{rx} contains different information always identified with the "rx" subscript, such as the provider identifier P_{rx} or the service type s_{rx}. Finally, the received packet can be a publish one or a request of the service r.

III. MISSION SCENARIO AND SATELLITE MODEL

The evaluation of the OSADP behavior and performance is crucial to consider if the protocol is suitable for satellite networks. For that reason, a scenario that can provide relevant results needs to be conceived. As previously presented, the EO community has a great interest in developing satellite missions to monitor the Arctic region [1], [5]. Therefore, a scenario based on this type of mission would demonstrate the benefits of the OSADP in future EO missions. Furthermore, this approach follows the work presented in [11], which promotes inter-satellite communications in EO missions.

The scenario definition must identify the instruments, and satellites that typically are used for this kind of missions. In this scenario, a satellite is conceived as a platform that integrates an EO payload with other subsystems. Note that this work does not aim at evaluating the hardware impact of using federations, which was already discussed in [25].

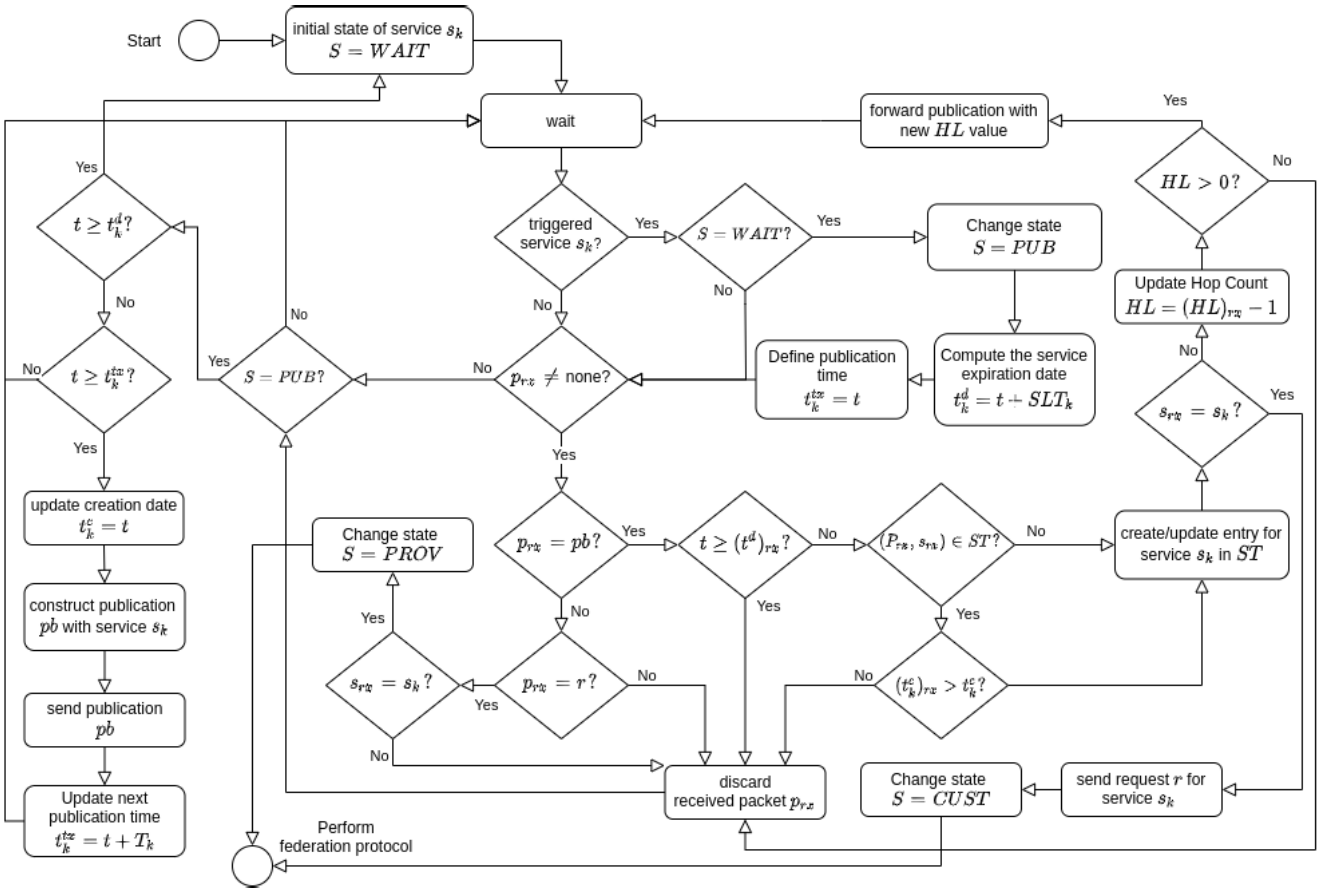

FIGURE 3. Flow diagram of the OSADP executed in a satellite.

Instead, it expects to evaluate its benefits in terms of increased download capacity. Therefore, the satellite model has focused only on three of those subsystems: the satellite-to-ground communication subsystem, the ISL subsystem, and the payload. Details on how these three subsystems have been modeled are presented in the following sections.

A. PAYLOAD TRAFFIC MODEL

The payload is the fundamental subsystem in a satellite, as it is all designed to achieve the mission goals. A payload generates data when the satellite ground track is over a target area. Therefore, it can be modeled as a Constant Bit Rate (CBR) application that periodically generates data over certain target areas. This case study has been focused on monitoring the ice status in the Arctic region. This region is delimited by the Arctic Circle, located at 66° of latitude (approximately). Thus, a satellite over the Arctic will generate data according to the payload that it is carrying. Figure 4 presents the Arctic region and the circle that delimits it (red line).

FIGURE 4. Map of the Arctic region, highlighted with red.

The ONION project conducted a survey and analysis of the different payloads that can be used for this type of mission [1]. The investigation concluded that the set of instruments that shall be used are a Synthetic Aperture Radar (SAR) at C- or X-band, a SAR Interferometer Altimeter (SIRAL), a Microwave Radiometer (MWR), a Microwave Radiation Imager (MWRI), an Advanced Microwave Scanning Radiometer (AMSR), Global Navigation Satellite System Reflectometer (GNSS-R), and a Radar Altimeter. Table 1 presents the payload data rates retrieved

TABLE 1. Payload model parameters.

	Data Rate
SAR-C	10.1 Mbps
SAR-X	35.5 Mbps
SIRAL	10.1 Mbps
AMSR	87.4 kbps
Radar Altimeter	35.0 kbps
MWR	10.6 kbps
MWRI	100.0 kbps
GNSS-R	16.8 kbps

from the Observing Systems Capability Analysis and Review (OSCAR)[1] database [26].

B. SATELLITE CANDIDATES

The selection of the spacecraft that should compose the scenario has been deeply studied. In order to demonstrate the benefits of using the OSADP in current and future satellite missions, only satellites that are currently in-orbit have been selected. Moreover, these satellites must have been conceived to observe the ice status in the Arctic region, and thus being able to carry some of the previous payloads. These satellites must follow a polar orbit (i.e. roughly 98° orbit inclination). Considering the heterogeneity of federation approaches, spacecraft from different national agencies and dimensions have been considered. Table 2 presents the list of those EO satellites that have been selected using the OSCAR database again [26]. Note that this table also presents the orbital elements of each satellite, which have been extracted from the CelesTrak[2] database [27].

The impact of the network disruption or fragmentation due to deploying a limited number of satellites was highlighted in a previous work of the authors [11]. This common situation in satellite networks provokes that it is not always possible to ensure a connection between two remote satellites. Therefore, to avoid that this phenomena could impact the evaluation of the proposed OSADP a mega-constellation has been included as a network backbone. Using this massive satellite system, the connectivity of the network is improved and thus the fragmentation of the network is mitigated. A detailed analysis of different mega-constellations proposals is presented in [17]. Reviewing the performance of each architecture, the Telesat approach has been selected because it provides the highest connectivity with less number of satellites. Details about the constellation architecture are presented in Table 3.

C. DOWNLOAD TRAFFIC MODEL

In satellite missions, the ground segment provides the communications interface with the satellite using a network of ground stations. This infrastructure enables the transmission of telecommands, and the reception of data from the satellites. This interface is available only when the satellite is in line-of-sight of the ground station (i.e. a *satellite pass*). The duration of this pass drives the amount of data that can be downloaded, and thus the entire traffic download of the satellite system. Therefore, the ground segment must be modeled properly.

This work aims at evaluating the behavior and performance of the OSADP design. A proper configuration of the ground segment that promotes satellite passes, and thus the possibility to publish downlink opportunities, would facilitate this analysis. For this reason, current operative ground stations have been selected considering their location. Table 4 details the list of the selected ground stations, and Figure 5 places them on the surface of the Earth, showing a large ground segment around the globe.

An area around the ground station represents the region over which a satellite pass is feasible. Thus, when a satellite ground track passes over this ground station area, the satellite

[1]OSCAR database has mission information and satellite characteristics.

[2]CelesTrak database has in-orbit spacecraft Two Element Lines (TLE). Accessed on 24th July 2018.

TABLE 2. Earth observation satellite features used to perform the analysis.

Identifier	Satellite	Operator	Payload	Semi-major axis	Eccentricity	Inclination	RAAN*	AP**	Mean Anomaly
Ice Observation Satellites									
sat-0	TanDEM-X	DLR	SAR-X	6886 km	0.0002	97.5°	62.0°	0.0°	271.0°
sat-1	TerraSAR-X	DLR	SAR-X	6886 km	0.0002	97.4°	58.0°	0.0°	46.0°
sat-2	SEOSAR/Paz	Hisdesat	SAR-X	6885 km	0.0002	97.4°	66.0°	0.0°	121.1°
sat-3	Sentinel-1A	ESA	SAR-C	7064 km	0.0001	98.2°	57.0°	0.0°	287.0°
sat-4	RadarSat-2	MDA	SAR-C	7169 km	0.0001	98.6°	56.5°	0.0°	27.3°
sat-5	RISAT-1	ISRO	SAR-C	6917 km	0.0005	97.6°	58.1°	0.0°	218.8°
sat-6	GaoFen-3	CNSA	SAR-C	7129 km	0.00007	98.4°	58.5°	0.0°	303.0°
sat-7	Sentinel-3A	ESA	MWR	7181 km	0.0001	98.6°	117.0°	0.0°	261.7°
sat-8	CryoSat-2	ESA	SIRAL	7088 km	0.0009	92.0°	261.2°	0.0°	147.5°
sat-9	Aqua	NASA	AMSR-E	7076 km	0.00001	98.2°	351.3°	0.0°	293.0°
sat-10	FY-3D	CNSA	MWRI	7207 km	0.0002	98.8°	351.6°	0.0°	348.0°
sat-11	HY-2A	CNSA	Radar Alt	7335 km	0.00003	99.3°	60.0°	0.0°	293.2°
sat-12	SARAL	CNES and ISRO	Radar Alt	7171 km	0.0002	98.5°	237.3°	0.0°	213.8°

*Right Ascension of the Ascending Node; **Argument of Periapsis

TABLE 3. Telesat Mega-constellation characteristics.

Plane Type	Planes	a^*	i^{**}	e^{***}	Sat/plane
Type 1	6	7371 km	99.5º	0.0	12
Type 2	6	7571 km	37.4º	0.0	9

*Semi-major axis; **Inclination; ***Eccentricity

TABLE 4. Ground stations locations that conforms the ground segment in the simulation, and the World Geodetic System 84 (WGS84) as the Earth model.

Ground Station	Country	Latitude	Longitude
Beijing	China	40.5º N	116.9º E
KaShi	China	39.5º N	76.0º E
Kumamoto	Japan	32.8º N	130.9º E
Libreville	Gabon	0.4º N	9.6º E
Ohio	USA	40.0º N	83.0º W
Matera	Italy	40.7º N	16.7º E
Neustrelitz	Germany	53.4º N	13.1º E
Prince Albert	Canada	53.2º N	105.9º W
Shadnagar	India	17.0º N	78.2º E
SanYa	China	18.3º N	109.3º E
Carnavaron	Australia	24.9º S	113.7º E
Shoal Bay	Australia	12.4º S	131.0º E
Chilton	United Kingdom	51.6º N	1.3º W
Addis Ababa	Ethiopia	9.0º N	38.8º E
Oregon	USA	45.5º N	122.7º W
Inuvik	Canada	68.3º N	133.6º W
Chetumal	Mexico	18.5º N	88.3º W
Malargüe	Argentina	35.5º S	69.6º W
Kourou	French Guyana	5.2º N	52.8º W
Cuidaba	Brazil	15.6º S	56.1º W
Hartebeesthoek	South Africa	25.9º S	27.7º E
Tidbinbilla	Australia	35.4º S	149.0º E
M'Bour	Senegal	14.4º N	16.9º W
Irkutsk	Russia	52.2º N	104.3º E
Magadan	Russia	59.6º N	150.8º E
Moscow	Russia	55.7º N	37.6º E
Svalbard	Norwegia	78.2º N	15.4º E
Kiruna	Svergie	67.9º N	21.0º E
Alaska	USA	64.6º N	147.5º W
Troll	Antarctica	72.0º S	2.5º E

downloads data following a CBR transmission. The dimensions of this downlink region directly depend on the minimum elevation angle (α) above the horizon at which the ground station can communicate with the satellite. The minimum value of this parameter is achieved at the maximum distance (r_{max}) that satisfies the link budget between the satellite and the ground station. Figure 6 presents a plot illustrating these two parameters, and the area over which the satellite downloads data (blue surface).

The definition of the link budget is determined by the transmission and reception features of each node (i.e. the satellite and the ground station). Transceivers working at multiple frequencies have been used in the past missions. From all of them, the S-band transceiver has been founded as a primary

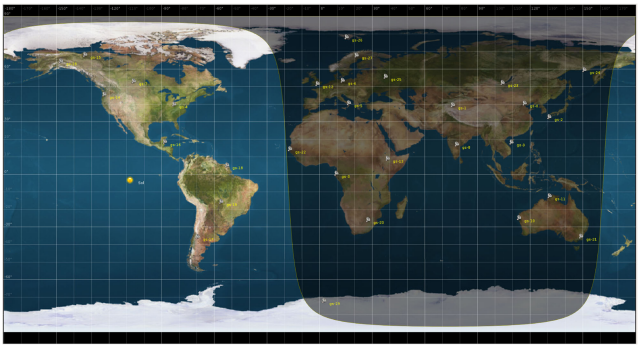

FIGURE 5. Location of the ground stations on the Earth.

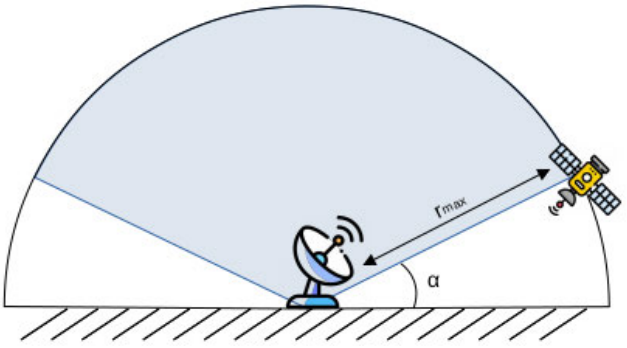

FIGURE 6. Ground station model with the corresponding communication area (gray surface).

solution for satellite platforms. Although each Commercial Off-The-Shelf (COTS) transceiver has its own characteristics, all of them can provide at least 1 Mbps of data rate [28]–[31]. A link budget analysis with a S-band transceiver is presented in [32]. Applying specific coding and modulation techniques and considering atmospheric effects, the achieved maximum distance and data rate are 1392 km and 3.4 Mbps respectively. Considering that the minimum COTS transceiver provides a smaller data rate, the maximum distance of this analysis can be incremented. Therefore, following the formulation of [32], a common S-band transceiver for all the satellites is selected, which transmits at 1 Mbps and has a maximum distance of 2500 km. Note that although Telesat satellites work at Ka-band [17], it has been preferred to "virtually" equip them with the S-band transceiver to unify the downlink capabilities.

Considering this maximum distance value, Table 5 presents the corresponding minimum elevation angles of each satellite, selected in Section III-B. The downlink regions for each satellite are computed with these angle thresholds. Figure 7 presents these regions for the SEOSAR/Paz satellite as an example. For those satellites that are not placed on these downlink regions, they can still transmit data using the ISN or become part as intermediate nodes.

D. INTER SATELLITE LINK MODEL

In this scenario, satellite platforms have satellite-to-satellite communication capabilities, thanks to ISL subsystems. This

TABLE 5. Minimum elevation angle of each satellite.

Satellite	Altitude [km]	Max. distance [km]	α [°]*
TanDEM-X	515	2500	11.89
TerraSAR-X	515		11.89
SEOSAR/Paz	514		11.86
Sentinell-1A	693		16.09
RadarSat-2	798		18.61
RISAT-1	546		12.62
GaoFen-3	758		17.65
Sentinel-3A	810		18.91
CryoSat-2	717		16.67
Aqua	705		16.38
FY-3D	836		19.54
HY-2A	964		22.68
SARAL	800		18.66
Telesat Type-1	1000		23.58
Telesat Type-2	1200		28.69

* Minimum elevation angle

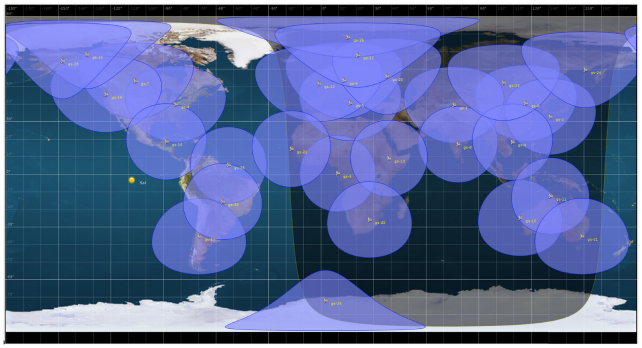

FIGURE 7. Downlink regions for SEOSAR/Paz satellite.

technology has already been deployed in large satellite missions (e.g. Iridium constellation [33]), and currently is being demonstrated for smaller platforms, such as CubeSats. The Gomspace GOMX-4 mission established a S-band ISL between two 6U CubeSats at a distance of 500 km. The in-orbit results [34] show that further ranges can be achieved combining multiple modulations and different transmission power profiles. Additionally, the FSSCat mission [5] plans to execute two payloads that perform different ISLs. The FSS Experiment (FSSExp) payload [16] uses a Radio Frequency (RF) ISL in Ultra High Frequency (UHF) band for a low data rate link between two 6U CubeSats, achieving 9.6 kbps at 1000 km of maximum distance, while the Optical ISL (O-ISL) payload [35] aims at demonstrating the feasibility of optical technology for CubeSats.

An ISL subsystem model can thus be characterized mainly with three parameters: the maximum communication distance d_{max},[3] the transmission data rate achieved at this distance Rb, and the radiation pattern or direction. As the results achieved in [11] highlight, the ideal ISL subsystem would provide great data rates, large communication ranges, and transmitting through an omnidirectional pattern. With these characteristics, it would be possible to have a system that provides fast transmission and high connectivity. Unfortunately, these characteristics cannot be achieved using a single subsystem. Nevertheless, the combination of multiple ones can address this challenge.

This approach is considered in this scenario. In particular, different ISL subsystems are combined to create two communications planes: the control, and the data planes. Software Defined Networks (SDN) and 5G networks have been working on this concept some time ago [36] highlighting the benefits of using these two planes. Combining decoupled and independent planes it is then possible to isolate network managing tasks and traffic, which is used to optimize the data transmission on the other plane. Note also that in [25] FSS commands and scientific data are differentiated, implicitly working with these two planes.

The control plane provides a communications channel for those packets that manage the network. Typically, these kinds of packets are composed of small byte structures, and they do not require high transmission data rates. Additionally, a subsystem that provides a large communications distance is necessary to increase the connectivity. In this direction, transceivers that work at Very High Frequency (VHF) and UHF would suffer less attenuation due to the signal propagation. Although the International Telecommunication Union Radiocommunication (ITU-R) sector does not consider ISL frequency bands below 22 GHz, some satellite missions have already used these previous bands for this purpose [8]. The continued interest in this field should encourage the discussion of the corresponding coordination in upcoming World Radiocommunication Conferences (WRC).

Taking into consideration these requirements, the ISL for the control plane can be implemented with a monopole antenna, and modulation techniques applied in Low-Power Wide-Area Networks (LPWAN) [38]. A large family of technologies have been developed for LPWAN, standing out the Narrow-Band Internet of Things (NB-IoT) [39]. The NB-IoT is conceived to provide considerable data rate with low power consumption, and for indoor communications with high density nodes. Its standardization, performed by the 3rd Generation Partnership Project (3GPP) [40], has expanded its use in current IoT ground networks. However, this technology has not been yet evaluated in space missions. On the other hands, the Long Range (LoRa) technology [41] has been evaluated and studied for CubeSats missions [42]–[45]. LoRa works at unlicensed UHF band, and it is designed to provide different low data profiles at long ranges. It seems thus suitable for the ISL subsystem responsible of the control plane.

The data plane provides a communications channel to transmit the generated data from the payloads. This data flow requires a communication link with a high data rate. In order to satisfy this requirement, an ISL subsystem based on a directive antenna would provide enough power at large distances, by specifically pointing to the neighbor satellite.

[3]Note that r_{max} has been used for satellite-to-ground communications, and d_{max} for satellite-to-satellite communications.

In this case, the coordinated ISL bands of ITU-R suit perfectly for this purpose, such as the Ka-band. This band has started to be used in spacecraft configurations, such as the ones of the Starlink mega-constellation [46]. These spacecraft use a four phased array antenna which generate different beams of 2.5° beamwidth [47].

The combination of both planes provides a satellite-to-satellite communications interface with high connectivity, large range, and great data rate. In particular, a satellite uses the control plane to manage the network and also to detect the pointing direction of the data plane ISL subsystem. This would be feasible if the satellite is able to predict the relative position of its neighbors, as authors in [48] proposes. Additionally, authors in [25] remarks that current attitude actuators are accurate and fast enough to achieve this system.

Different link budgets of both planes are presented in Tables 6 and 7. These link budgets have been performed considering the previous possible configurations, and for two cases: one in which both satellites are close (1500 km), and another on where they are far away (3000 km). The link budgets of the control plane have been based on the LoRa SX-1261X chip characteristics [37]. However, due to private information, the Forward Correction Code (FEC) gain has not been considered in the link budgets. The link budgets related to the data planes have been based on the downlink and uplink transceiver characteristics of Telesat satellite, provided in [17]. In particular, the Effective Isotropically Radiated Power (EIRP), the modulation, and other aspects have been considered to compute the link budgets. These budgets remark that satellite-to-satellite communications can be established at 1500 km and at 3000 km, modifying properly the modulation and bandwidth. Specifically, the ISL subsystem for the control plane offers 5.5 kbps at 1500 km, and 1.8 kbps at 3000 km, while it offers for the data plane 104.1 Mbps at 1500 km and 1.1 Mbps at 3000 km. Taking into consideration these values, a type of ISL subsystem with a maximum distance of 1500 km and different rates of 1 Mbps, 10 Mbps, and 100 Mbps has been considered for this study. Moreover, another subsystem providing 1 Mbps at 1500 km, 2500 km, and 3000 km has also been considered.

TABLE 6. Link budgets for close and far cases of the ISL for the control plane.

Parameter	Close case	Far case	Unit
Frequency *	868	868	MHz
Bandwidth *	125	125	kHz
Transmitted Power	30	30	dBm
Tx. Antenna Gain	1	1	dB
EIRP	31	31	dBm
Spreading Factor *	7	9	
Coding Rate *	4/5	4/5	bps/Hz
Path Distance	1500	3000	km
Free Space Loss	154.7	160.75	dB
Rx. Antenna Gain	1	1	dB
Rx. Power	-122.7	-128.8	dB
Sensitivity *	-123	-129	dB
Margin **	0.3	0.3	dB
Data Rate *	5.5	1.8	kbps

* Retrieved from LoRa SX-1261X [37]; ** FEC gain is not considered

TABLE 7. Link budgets for close and far cases of the ISL for the data plane.

Parameter	Close case	Far case	Unit
Frequency **	23.3	23.3	GHz
Bandwidth	75	0.8	MHz
EIRP *	36	36	dBW
Modulation *	16APSK	16APSK	
Coding Rate *	28/45	28/45	
Spectral efficiency *	2.23	2.23	bps/Hz
Path Distance	1500	3000	km
Free Space Loss	183.3	189.3	dB
Rx. Antenna Gain *	31.8	31.8	dB
Rx. System Temperature *	285.3	285.3	K
Rx. Power	-115.5	-121.5	dBW
Rx. SNR	9.8	23.5	dB
Req. Eb/N0 *	4.6	4.6	dB
Req. SNR	6.0	6.0	dB
Link Margin	3.8	17.5	dB
Data Rate	104.1	1.1	Mbps

* Retrieved from [17]; ** Inter-Satellite band coordinated by ITU

IV. SIMULATION ENGINE AND IMPLEMENTATION

The analysis presented in this work has been performed with a simulation engine specifically developed to execute satellite networks [49]. This engine is implemented on top of the Network Simulator version 3 (NS-3) [50] which is an event-based simulation engine core. In particular, it provides mechanisms to manage scheduled events, which correspond to satellite actions (e.g. packet transmission and reception).

The scenario definition in this simulator is centered on the satellites and their subsystems. Taking the models presented in Section III, a simulation structure has been conceived accordingly. Figure 8 presents the Unified Modeling Language (UML) diagram of the different classes that represent a satellite. The NS-3 simulator defines a `Node` as an entity that has a set of `Applications` and protocols. In this case, the main application is the `SatelliteApplication`. This one manages the operations of the satellite, deciding when an action has to be executed. A `Scheduler` provides support notifying when the satellite ground track is over a specific area. Therefore, thanks to these notifications, the satellite generates data with the `Payload` application or downloads data with the `TelemetryAndTelecommand` one. The exchange of data between those two applications is performed using a `DataBuffer`. Note that these applications are implemented according to the models presented in Sections III-C and III-A.

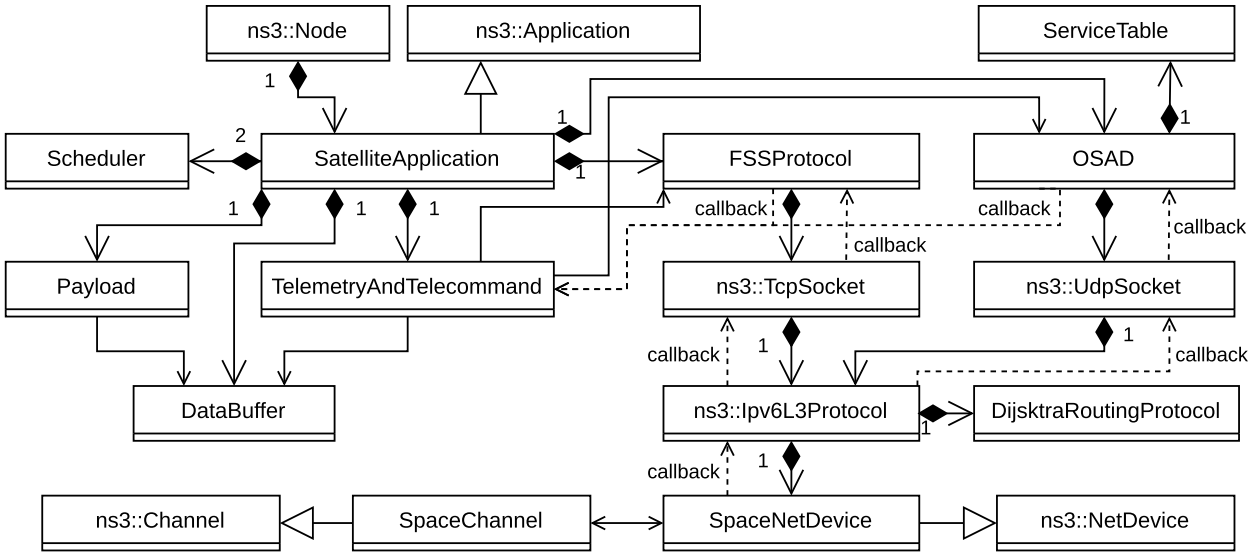

FIGURE 8. Simplified UML diagram of a satellite in the simulation.

The OSADP is implemented in the `OSADP` class, with its corresponding `ServiceTable`. This protocol uses a User Datagram Protocol (UDP) socket because the reliability is not required during the publication of the service. Additionally, the `FSSProtocol` implements the federation protocol, presented in [16], that uses a Transport Control Protocol (TCP) socket because it is important to ensure that the data has been correctly propagated until the destination. Both types of sockets directly interact with the Internet Protocol version 6 (IPv6), which has a custom routing protocol based on the Dijkstra algorithm [51]. This work does not aim at evaluating the consequences of the selected routing protocol, and thus an ideal one has been considered. This protocol, however, may be evaluated with another routing protocol in future research, which may suit the requirements presented in [10]. Note that in this case, the provider identifier has been defined with the last three bytes of the IPv6 address.

The `TelemetryandTelecommand` not only manages the data download, it also triggers the publication in the `OSADP` class when the service is available (see previous Figure 3). A callback function is used in the opposite direction, i.e. when a publication is received with the `OSADP` class. In this last case, the `TelemetryandTelecommand` class deploys the federation using the `FSSProtocol`, which notifies about its status using different callback functions. The `SpaceNetDevice` and the `SpaceChannel` implement the discontinuity of the ISL due to satellite motions. As these classes are part of the simulator core, further information about their design can be found in this previous work [49].

This class structure is replicated for each satellite in the simulation scenario, previously presented in Section III-B. Note that the Telesat satellites do not have an EO payload, and neither the corresponding `Payload` class. Also the execution of the `OSADP` and `FSSProtocol` classes is configurable, enabling to select specific satellites that participate in the service publication and federations. With these features, the scenario has been simulated retrieving different metrics about the OSADP behavior.

V. RESULTS AND DISCUSSION

The OSADP behavior and performance is evaluated with the execution of the previous scenario. This scenario is executed during a simulated day (i.e. 86400 seconds), and different parameters related to satellite-to-satellite communications are configured. Additionally, satellites in this scenario that execute the OSADP transmit publications every 5 seconds, with 17 as HL. These parameters have been defined according to the dynamics of the networks, presented in Section V-B. The present analysis helps to understand how the OSADP improves the download capacity of the original EO satellites. For this reason, Section V-A discusses the initial capacity of only those satellites, highlighting an interesting progress margin. The stability of the topology is greatly impacted by the number of satellites. Therefore, a discussion of how the download capacity changes when the mega-constellation is used as a network backbone is addressed in Section V-B. After demonstrating the benefits of using this backbone, Section V-C goes deeper in evaluating the performance considering that satellites of the mega-constellation also publish the availability of their services.

A. SCENARIO STUDY

As it has been presented previously, EO satellites generate data when they are over the Arctic region, and download them when passing over a ground station. A data budget between the generated and downloaded data determines the storage capacity of the satellite. This budget is driven by the amount of time that each satellite passes over the target areas.

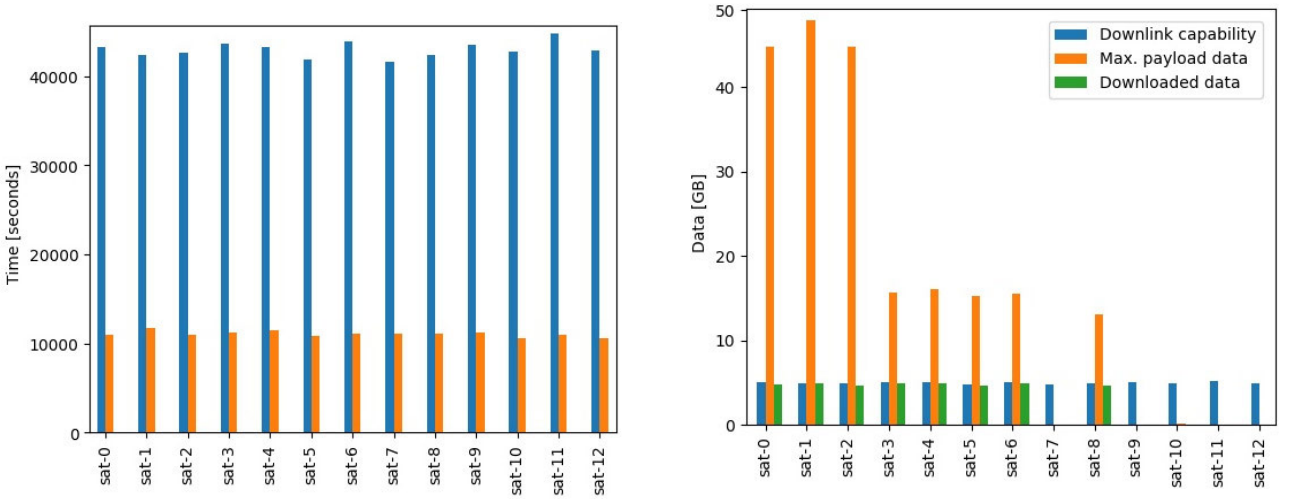

(a) Time over downlink (blue) and Arctic regions (orange)

(b) Downloaded (green) and generated data (orange) with respect the download capacity (blue)

FIGURE 9. **Time and data budgets of each EO satellite without using satellite-to-satellite communications.**

Figure 9a presents the accumulated time of each EO satellite over those areas after one simulated day. All of them pass around 12 hours per day over a ground station (blue bar), and have thus the opportunity to download up to 5.29 GB approximately. Note that this amount of time is very large because a large ground segment has been considered to promote downlink opportunities. Additionally, each satellite passes 3 hours per day (roughly) over the Arctic region, generating data according to its EO instrument.

Figure 9b shows the difference between time and data budgets. Satellites that carry payloads with greater data rate (i.e. from sat-0 to sat-6, and sat-8) generate more data (orange bar) than the one that they can download (blue bar). Although they are using all the downlink time to download its own data (green bar), this is not enough to avoid overloading their storage system. This result highlights that these SAR-based payloads cannot be executed over the entire Arctic zone, as it is the case in traditional monolithic satellite missions. Note that the satellites that carry these payloads are called "memory-overloaded EO satellites" during the rest of the results discussion. However, some satellites do not suffer from this problem (i.e. sat-7, and from sat-9 to sat-12), because they can download all the generated data. Additionally, these satellites have surplus downlink time that could be shared. These ones can thus offer this remaining capacity as a service that the memory-overloaded EO satellites could benefit.

The opportunity to share this unused time is achieved by enabling the satellite-to-satellite communications, and using the OSADP. Figure 10 presents a growth of the downloaded data when this interaction between satellites is enabled. In particular, this figure compares the system performance with respect to different ISL subsystems. These subsystems provide 1 Mbps of data rate at communications ranges (d) of 1500 km, 2500 km, and 3000 km. Clearly, the use of those

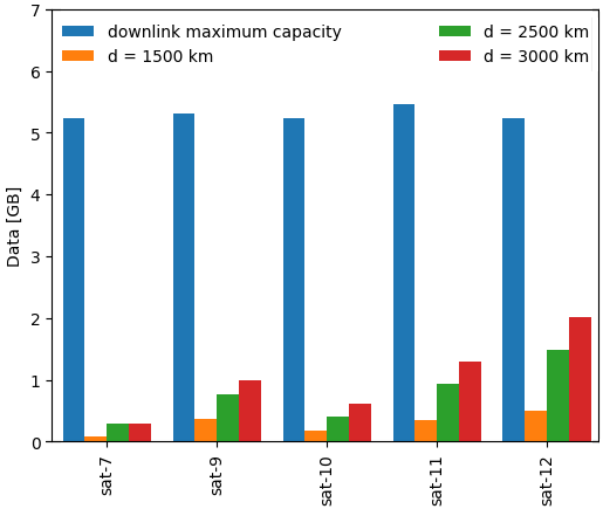

FIGURE 10. **Data budgets of EO satellites that provide downlink service with ISL subsystems of 1 Mbps data rate and different maximum ranges *d*.**

systems with larger range facilitates the propagation of the service publication, proliferating the federations. With these federations, the satellites download 5.24 GB per day more of the memory-overloaded EO satellites (in the 3000 km case).

These results demonstrate that the OSADP helps to establish satellite federations. Satellite resources are properly leveraged with these federations, and more data is downloaded. However, the previous figure also remarks that although using a range of 3000 km there is still unused downlink time. The network disruption is the cause of this behavior, which provokes that not all the customers can communicate with the service providers. This fragmentation behavior has been investigated in Delay/Disruptive Tolerant

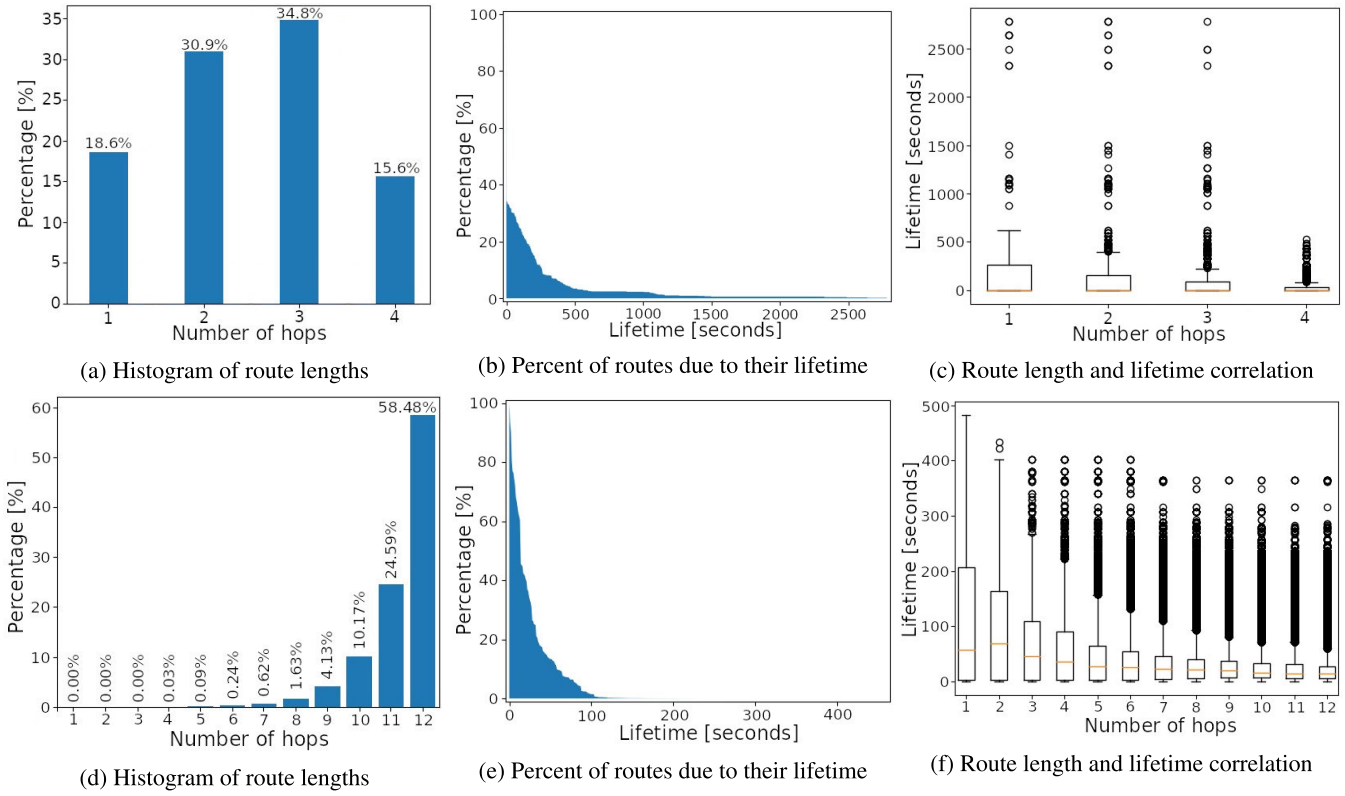

(a) Histogram of route lengths (b) Percent of routes due to their lifetime (c) Route length and lifetime correlation

(d) Histogram of route lengths (e) Percent of routes due to their lifetime (f) Route length and lifetime correlation

FIGURE 11. **Topology behavior without the Telesat mega-constellation (a, b, and c) and including it (d, e, and f).**

Networks [52], where a solution that takes advantage of the satellite orbit trajectory determinism was proposed. This is the case of the Contact Graph Routing (CGR) protocol [53], [54] which determines a route between a source and a destination over time using a contact plan. This plan is a scheduled sequence of contacts between all the satellites that compose the system. The route definition in this plan is commonly computed by a centralized infrastructure located on ground which evaluates relevant performance metrics [55]. The traditional criterion to determine the routes has been the minimization of the transport time from the satellite source to the destination. Nevertheless, other criteria have been considered to suit resource-constraint platforms. The Energy-aware CGR (E-CGR) [56] defines a route in the contact plan by taking in consideration the power status of all the satellites that determines the route. Other approaches [57] have defined algorithms to determine routes between satellites considering a link metric that merge multiple features (e.g. energy of satellites, time-varying satellite downlink contact capacity, and the differentiation for missions). Among the previous proposals, another approach has been focused on generating the contact plan autonomously by orbiting satellites [58].

Despite the different solutions on determining routes considering the network disruption, the use of a network backbone can also mitigate this phenomenon thanks to promote the connectivity with more satellites. This last approach has been used in the following simulations. This work does not aim at evaluating the consequences of network disruption in the proposed service notification, which may be discussed in future investigations. The remaining download capacity of the EO satellites may be leveraged by using a satellite backbone.

B. TOPOLOGY ANALYSIS

The integration of the Telesat mega-constellation as a network backbone increases considerably the number of satellites that participates in the network. As a result, the possibility to have multiple routes between a service provider and a customer becomes more probable. These routes are extended with additional intermediate satellites. Note that larger routes are susceptible to suffer more changes, making the entire topology more dynamic. Therefore, it is crucial to understand how the inclusion of the mega-constellation impacts on the topology dynamism.

Figure 11 presents the behavior of the topology before and after integrating the mega-constellation with the EO satellites (top and bottom figures respectively). Figures 11a and 11d present a histogram of the routes that are feasible according to the number of satellites that compose them (i.e. the route length). Figures 11b and 11e indicate the probability that a route is stable during (at least) a specific lapse of time, well-known as route lifetime. Finally, Figures 11c and 11f correlate this lifetime information with respect to the route

length, represented in box plots.[4] Note that these topology features were presented in details in this previous work [11].

Figures 11a, 11b, and 11c present the topology behavior when only EO satellites compose the satellite system (i.e. the one analyzed in Section V-A). In this scenario, the ISL subsystem has a maximum communications range of 1500 km. Figure 11a shows that only routes with less than four hops are feasible, being the most probable the routes with three hops (i.e. four satellites). This performance is related to the reduced number of satellites, just 12 spacecraft in this case. Additionally, some of these routes are quite stable reaching lifetime values up to 2500 seconds, as Figure 11b shows. Nevertheless, the majority have a short lifetime. This result is also presented in Figure 11c, where all the routes have commonly a short lifetime with some exceptional cases (represented in dots). This topology is thus driven by the network disruption, which produces short and unstable routes. As a result, producer and customer satellites cannot establish federations to download data.

These characteristics change when the mega-constellation is considered as part of the satellite system. Figure 11d shows that using the same ISL subsystem (i.e. 1500 km of range) the routes are more variable, but larger (up to 12 hops). Thanks to the increased number of satellites, the largest routes are more probable. This implies that the communications range is extended, being able to reach further satellites. Figure 11e highlights that the stability of a route has been homogenized with respect to the previous case, reducing the abrupt differences in some routes. However, this is still a high dynamic scenario, as Figure 11f remarks, because the most probable routes are the ones that have short lifetime. In summary, the use of the mega-constellation helps to expand the network diameter with larger routes, although they are more volatile.

As indicated in [59], the creation and destruction of ISLs changes the network topology over time. Each of those changes generates a *snapshot* of the topology which remains stable during a lapse of time. This stability duration is also another metric that helps to understand how dynamic a network is. Figure 12 shows the statistics of this snapshot duration in each of the previous cases (i.e. without and with mega-constellation). As a result, the use of the mega-constellation makes the topology more dynamic, generating more snapshots than in the case with only EO. Although the established federations could be broken due to the disappearance of a route, the possibility to expand the network becomes promising to establish federations.

It is important, however, to clarify if this improvement of the connectivity prevails over the variability of the network. For that reason, this scenario in which the EO satellites use the mega-constellation to forward publications is evaluated. The corresponding results are compared to the scenario in which only the EO satellite composes the satellite system,

[4]A box plot represents a distribution function as a box delimited by the third quartile and the first quartile. Additionally, the median is represented as a line in this box.

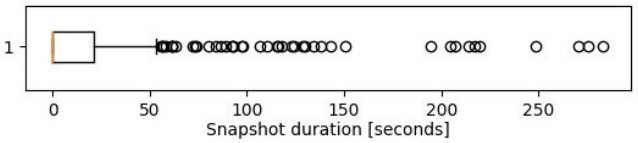

(a) Box plot (top) and samples (bottom) with EO satellites only

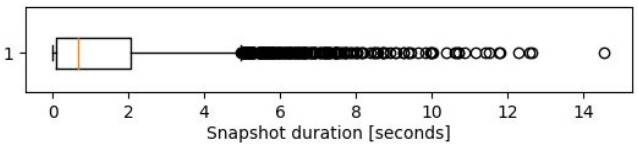

(b) Box plot (top) and samples (bottom) with mega-constellation

FIGURE 12. Duration between snapshots without Telesat mega-constellation (top) and with it (bottom).

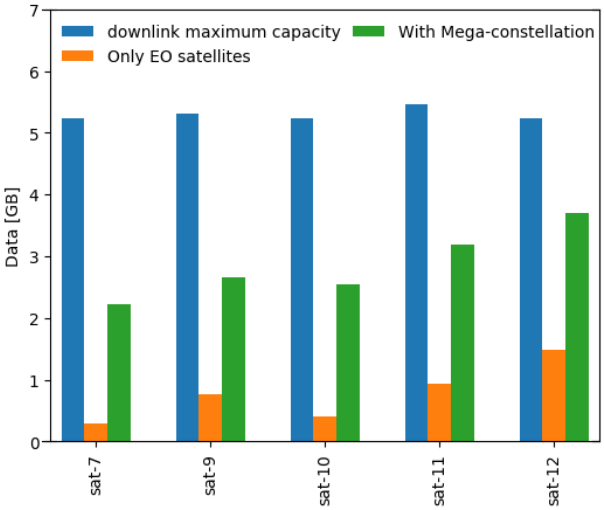

FIGURE 13. Data budgets of EO satellites that provide downlink service with ISL of $Rb = 1$ Mbps and $d_{max} = 2500$ km, with and without the mega-constellation.

presented in Section V-A. Figure 13 shows the downloaded data of those EO satellites that are not memory-overloaded, comparing both scenarios. In particular, the EO satellites that can provide the service download more data using the mega-constellation as backbone (green bar) than in the original case (orange bar). This remarks that although the network changes quickly, the possibility of having more and larger routes helps to download more data. Consequently, the use of the mega-constellation is beneficial. However, it remains still unused capacity (blue bar), which could be leveraged.

These results pose the question on what drives the use of this surplus capacity. For that purpose, the different actions that a satellite performs during a ground station pass are evaluated. During a pass, a satellite can perform three different actions: download its own data, publish the opportunity to download, or provide this downlink service to download data from others (i.e. it is federated). Figure 14 presents these three concepts in the form of time percents. These percents correspond to the average value computed with the time percents of each EO satellite. The study is thus focused on analyzing these averaged values which represent the behavior

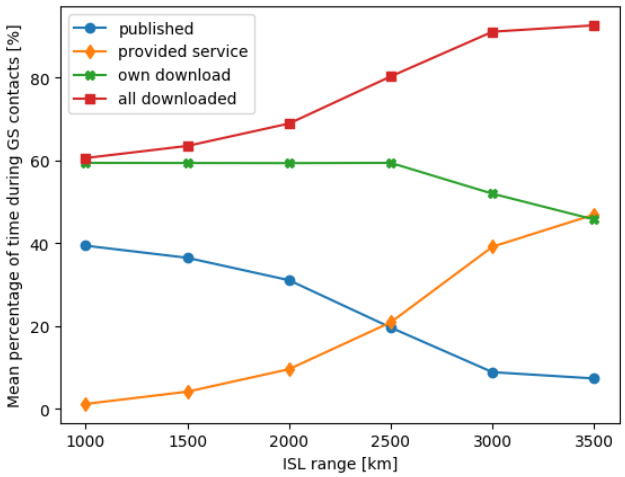

FIGURE 14. Average time percentages related to the downlink pass actions of all the EO satellite.

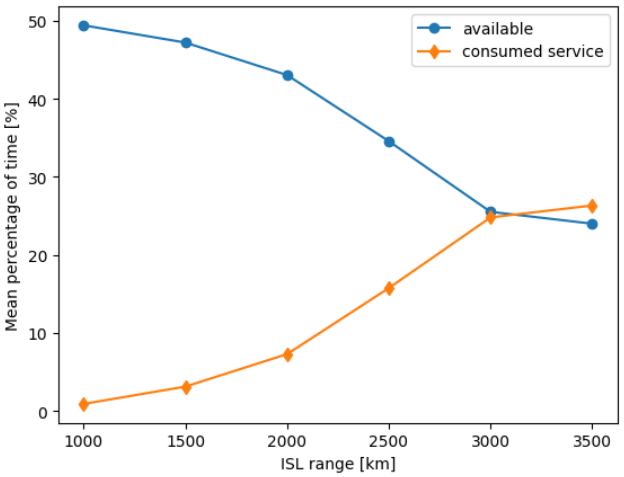

FIGURE 15. Average time percentage of inactivity (blue) and federated (orange) of the memory-overloaded EO satellite.

of an "average EO satellite". Specifically, how this average EO satellite uses its ground station pass depending on its ISL subsystem features is discussed. As indicated previously, the maximum range determines the expansion of the network, and thus the possibility to establish federations. For that reason, the time percent is plotted with respect to this feature.

Regarding the time used publishing downlink opportunities (dot-blue line in Figure 14), it decrements while the range increases. Increasing this range facilitates the establishment of federations, as diamond-orange line remarks with this growth of the time providing the service. Note that the EO satellites keep using the same time of a ground station pass to download its own data (cross-green line), until the range is 2500 km. At this moment, less time is used for this purpose, because the satellites have already downloaded it using federations. Although this decreases, the total time used downloading data (square-red line), its own and from the others, increases with the range. This result remarks that the ISL range allows leveraging the pass time by reducing the time during which the satellite is publishing, and thus downloading more data.

Considering that the saturated EO satellites should download data over federations, their activity would also drive the amounts of data that the entire system downloads. Specifically, if those satellites remain federated during all the time, this would signify that all data, susceptible to be downloaded, is indeed transferred. Therefore, the percentage of time during which an average satellite of those saturated does not transfer data is considered as a resulting metrics. The optimization of those satellites is thus characterized with these metrics. Figure 15 presents the evolution of this time percentage (dot-blue line) with respect to different ISL ranges. Note that this average satellite becomes more active when the range increases, due to the different federations that are established. In particular, this satellite passes from 12 hours per day (i.e. around 50% of a day) to 7 hours of inactivity (i.e. 29% of a day). Although in the best case (range 3500 km) the activity is considerably incremented, this average satellite still has some time that could use transferring data with federations. This result remarks that the download capacity of unsaturated EO satellites (i.e. sat-7 and form sat-9 to sat-12) is not enough to download all the generated data from the saturated ones. Therefore, this work goes deeper evaluating how this capacity increases while the mega-constellation satellites participate sharing their own downlink opportunities.

C. PARTICIPATION ANALYSIS

The participation of mega-constellation satellites by sharing downlink opportunities would provide more download capacity to the entire satellite system. With this approach, those saturated EO satellites could leverage the unused time transferring data with new federations. However, it is important to clarify how many of those mega-constellation satellites are needed to reach the maximum activity of the saturated ones. Thus, this section presents a study of the download capacity evolution with respect to the number of satellites from the mega-constellation sharing the service. Different groups of those satellites have been analyzed in different simulations, selected randomly of the entire constellation. Therefore, multiple simulations per group have been performed, retrieving at the end an average behavior (represented in all the figures as a slashed line). Note that those satellites that are not included as publishers of the service, they take part of the network backbone to keep the same connectivity as before.

Figure 16a plots the bytes downloaded per day of the entire system depending on the number of mega-constellation satellites that publish the service. As remarked in the previous results, the communications range of the ISL subsystem is one of the parameters that drives the data download. Therefore, this metric is compared to ranges of 1500 km (blue line), 2500 km (green line), and 3000 km (red line). In those cases, the data rate of the ISL subsystem remains equal to 1 Mbps.

If no satellite from the mega-constellation publishes the service, they conform the network backbone as in Section V-B. Consequently, the resulting downloaded data is

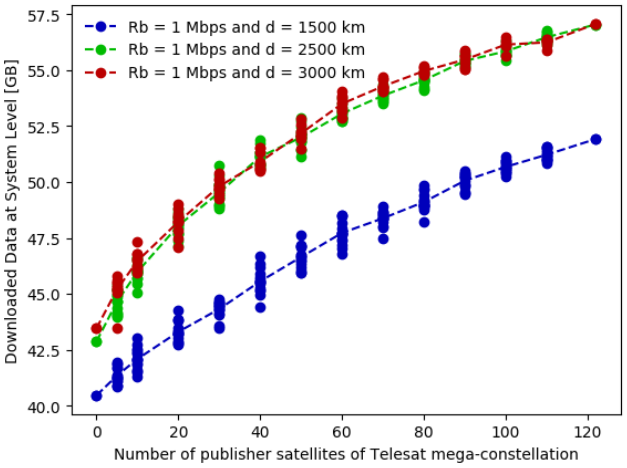

(a) Downloaded data depending on the publisher satellites

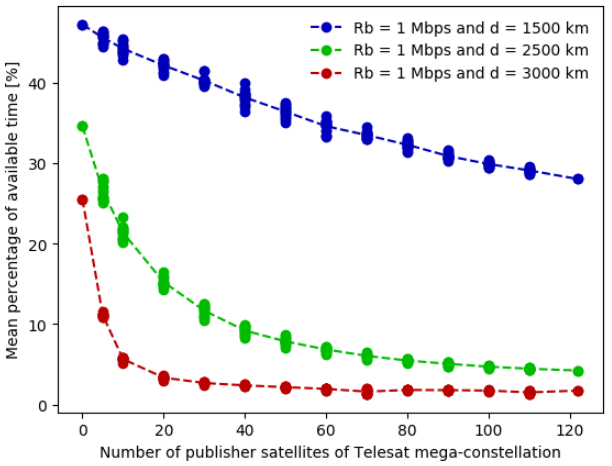

(b) Average available time percent per day of memory-overloaded EO satellites with respect to the publisher satellites

FIGURE 16. Downloaded data and average available time percent of the memory-overloaded EO satellites per day according to the publisher satellites and ISL subsystems with Rb = 1 Mbps and different maximum ranges d_{max}. Simulations conducted in a intel-i7 computer with 16 GB of DDR4 memory, and spending between 30 minutes up to 40 hours per simulation.

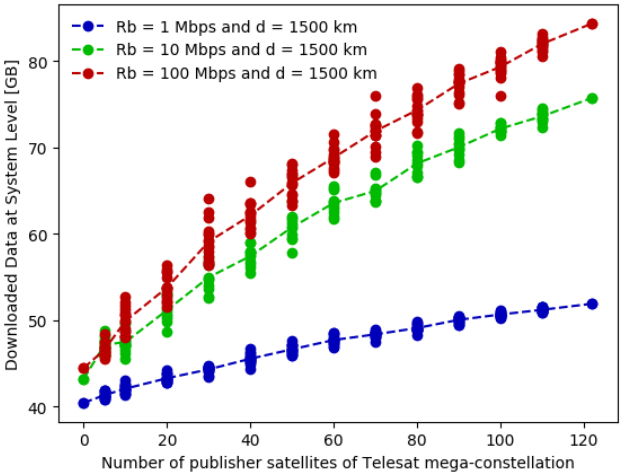

(a) Downloaded data with respect to the number of publishers and ISL maximum ranges

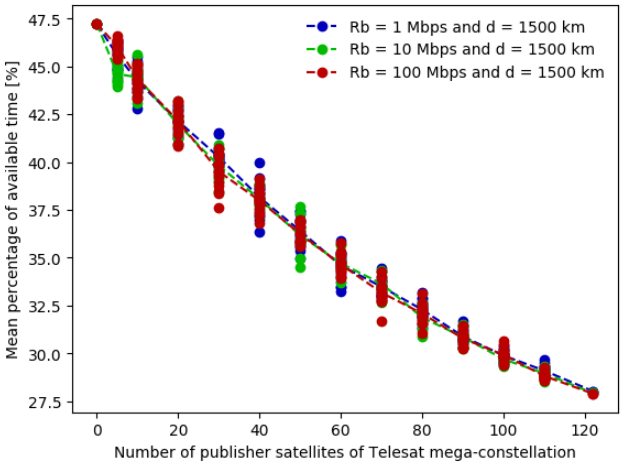

(b) ISL of 1 Mbps and 2500 km as range

FIGURE 17. Downloaded data and time percentage of saturated EO satellites per day according to the publisher satellites and ISL subsystems with d_{max} = 1500 km Mbps and different data rates Rb. Simulations conducted in a intel-i7 computer with 16 GB of DDR4 memory, and spending between 30 minutes up to 40 hours per simulation.

the same as in Figure 13, growing with larger ranges. While the more publishers start to participate, the downloaded data increases following a logarithmic growth in the three cases. This behavior is correlated with Figure 16b which presents the time percentage per day of the average saturated satellite that is not being used to transfer data (as in Figure 15). As expected, this performance metric decreases while the number of publishers increases. In particular, when the range is 1500 km the unused time is reduced from 11 hours to 8 hours per day (approximately), having still some unused time. This curve changes considerably for larger ISL ranges, such as 2500 and 3000 km. In particular, the value trend follows a logarithmic curve, reaching a minimum of 45 minutes per day of inactivity (best case). This is also reflected in previous Figure 16a where the amount of downloaded data is bounded until a maximum value, because the saturated satellites do not have more time to keep downloading data with federations. In this case, the entire satellite system can download 51.92 GB, 57.04 GB, and 56.11 GB (respectively). This corresponds to an increase of 34%, 47%, and 45% of the number of downloaded bytes with respect to the original case (only EO without satellite-to-satellite communications).

One of the resulting features of this topology (presented in Section V-B) is that the routes are abundant and large, but also short in lifetime. Therefore, federations are established also shortly, being necessary to leverage the time while they are stable. Therefore, the data rate of the ISL subsystem can play an important role. Specifically, more data can

be exchanged during the same lapse of time with greater data rates. Figure 17 presents thus a study on how the data download is impacted with three ISL subsystems providing 1 Mbps, 10 Mbps, and 100 Mbps at 1500 km of range. At the first sight, the amount of downloaded data has increased considerably, reaching greater values than in the previous case (modifying the distances). Additionally, the improvement between the different data rates is not linear. Indeed, there is less improvement passing from 10 Mbps to 100Mbps, rather than from 1 Mbps to 10 Mbps. This situation appears because although the ISL data rate grows, the downlink data rate remains always to 1 Mbps. Thus, the bottleneck would be this downlink interface. There is, however, an important conclusion in these results: spreading the data over the entire satellite system is beneficial, because each satellite will then download the data during its downlink passes.

Note that the inactive time percentage of the saturated satellites follows in all the cases the same curve in Figure 17b, which is indeed the same as the blue line in Figure 16b. This reinforces the concept that **the distance is the unique parameter of the ISL subsystem that can modify the activity of those saturated satellites**. It is not the case of the downloaded data, which is affected by the range and the data rate. Note that this also indicates that there is still margin to improve if an ISL that provides high data rate and large range is installed in the satellite. These configurations download a maximum of 51.92 GB, 75.74 GB, and 84.36 GB respectively. This corresponds to a growth of 34%, 95%, and 118% with respect to the original case.

In conclusion, the use of the OSADP enables downloading more data in all cases, being evident that the improvement is larger when more satellites participate sharing the service. Additionally, the results demonstrate that increasing the ISL range enables to improve the connectivity, and thus the use of time that saturated satellites remain inactive. However, ISL subsystems with greater data rates better leverages the temporal connections than those with larger ranges. **To increase the amount of downloaded data, the enhancement of ISL data rate seems to be more beneficial**. This is the case for those satellite missions that are limited in the downlink capacity, and it is intended to improve it.

VI. CONCLUSION AND FUTURE RESEARCH

Nowadays, there is a growing demand on new services with high temporal and spatial resolutions to monitor the Arctic region [1]. Monolithic satellite missions would have problems downloading the large amount of generated data. This would result in the loss of important information, and thus mechanisms to address this situation must be conceived. The increase of the download capacity of the satellite system is a promising option to be developed. In this regard, the FSS concept can be beneficial by promoting collaborations (federations) between satellites. These collaborations aim at consuming unused resources by other satellites as services, such as downlink capacity. Moreover, the IoSat paradigm extends this concept event farther by proposing temporal networks of satellites to establish federations between remote satellites.

One of the challenges of these paradigms is the notification of the available services. For that reason, this work has presented the OSADP, by which a satellite publishes its available services following a proper dissemination in the network. This dissemination mechanism is similar to the one presented in the BATMAN protocol [23] for the OGM, bounding the regions of the network to be forwarded. A satellite that receives this publication retrieves information about the available service, and it can decide to request it using a federation or discard the notification in case the satellite is not interested. The design of the protocol has been detailed in this work, presenting all its features, such as packet format, and the publication flow diagram.

To evaluate the OSADP design a realistic scenario composed of EO satellites that monitor the Arctic region has been defined. These satellites are equipped with payloads commonly used to observe the ice status, such as SAR and MWRs. A large ground segment has been defined to provide enough downlink opportunities to be published, and additionally the Telesat mega-constellation has been integrated as a network backbone. The downlink areas have been properly modeled according to current technologies used in satellite missions. Furthermore, different ISL subsystems have been considered to evaluate its impact on the OSADP.

The results presented in this work demonstrate that the OSADP enables the establishment of federations, and greatly increases the amount of downloaded data by the entire system. Specifically, executing this protocol with only the EO satellites allows downloading 7% more than not using it. In this case, the potential benefits of applying this solution are limited by the network disruption dissociated to the small number of satellites deployed. Despite this limitation, the use of the OSADP in current satellite missions improves the downlink capacity. To mitigate this situation and fully evaluate the potential of the OSADP, a satellite backbone has been integrated. Assuming a Telesat like mega-constellation–with maximum communications ranges from 1500 km to 3000 km, and a data rate from 1 Mbps to 100 Mbps–is included as network backbone, the system can download up to 15% (depending on the ISL characteristics) than the original case. Finally, if the mega-constellation publishes its downlink opportunities, the downloaded data growth is 118%, i.e. the overall downloaded data is more than doubled.

As ISL subsystems with different communications ranges, and data rates have been used, the study also provides information about how these characteristics suit satellite networks. These networks are characterized by being greatly variable, having considerable changes on the different links that compose the network. The retrieved results remark that an ISL with greater data rate than larger range better matches this kind of network. In particular, large data rate allows optimizing the temporal links by exchanging more data, and thus downloading more data for the entire system. Therefore, for the purpose of download capacity, ISL with a high data

rate should be promoted. For other goals (e.g. to minimize latency), a different analysis must be conducted.

All these results demonstrate that the proposed protocol can improve current and future EO missions by downloading more data. As compared to the traditional solution of increasing the number of ground stations, the OSADP reduces the cost of the downloaded data (i.e. cost per byte), as the same ground segment. Furthermore, the growth on the downlink opportunities enables to retrieve the generated data faster than in the traditional case. Finally, the OSADP enables to optimize the satellite resources by notifying the available ones to establish federations, as the FSS proposal.

Despite all these benefits, the potential of the OSADP is limited by the network disruption. As previously discussed, the protocol is originally conceived to provide mechanisms to leverage the opportunity to consume services that remain available during lapses of time. Therefore, the protocol definition does not take in consideration the network disruption. Nevertheless, this fragmentation could miss the opportunity to consume an available service due to the lack of a route. In this regard, the application of disruptive-tolerant mechanisms in the OSADP may be interesting protocol extensions to be addressed in future investigations. These improvements would enhance its features and allow it to achieve its maximum performance, which has been presented with the satellite backbone case.

REFERENCES

[1] E. Alarcon *et al.*, "Design and optimization of a polar satellite mission to complement the copernicus system," *IEEE Access*, vol. 6, pp. 34777–34789, 2018.
[2] J. Awange and J. Kiema, "Disaster monitoring and management," in *Environmental Geoinformatics*. Springer, 2019, pp. 533–578.
[3] E. Lancheros, A. Camps, H. Park, P. Sicard, A. Mangin, H. Matevosyan, and I. Lluch, "Gaps analysis and requirements specification for the evolution of copernicus system for polar regions monitoring: Addressing the challenges in the horizon 2020–2030," *Remote Sens.*, vol. 10, no. 7, p. 1098, Jul. 2018.
[4] J. F. Munoz-Martin, L. F. Capon, J. A. Ruiz-de-Azua, and A. Camps, "The flexible microwave payload-2: A SDR-based GNSS-reflectometer and L-Band radiometer for CubeSats," *IEEE J. Sel. Topics Appl. Earth Observ. Remote Sens.*, vol. 13, pp. 1298–1311, Mar. 2020.
[5] A. Camps, A. Golkar, A. Gutierrez, J. A. Ruiz-de-Azua, J. F. Munoz-Martin, L. Fernandez, C. Diez, A. Aguilella, S. Briatore, R. Akhtyamov, and N. Garzaniti, "Fsscat, the 2017 copernicus masters 'ESA sentinel small satellite challenge' winner: A federated polar and soil moisture tandem mission based on 6u cubesats," in *Proc. IEEE Int. Geosci. Remote Sens. Symp. IGARSS*, Jul. 2018, pp. 8285–8287.
[6] M. Esposito, S. Conticello, M. Pastena, and B. Domínguez, "In-orbit demonstration of artificial intelligence applied to hyperspectral and thermal sensing from space," *Proc. SPIE*, vol. 11131, Aug. 2019, Art. no. 111310C.
[7] D. Selva, A. Golkar, O. Korobova, I. L. I. Cruz, P. Collopy, and O. L. de Weck, "Distributed Earth satellite systems: What is needed to move forward?" *J. Aerosp. Inf. Syst.*, vol. 14, no. 8, pp. 412–438, Jan. 2017.
[8] R. Radhakrishnan, W. W. Edmonson, F. Afghah, R. M. Rodriguez-Osorio, F. Pinto, and S. C. Burleigh, "Survey of inter-satellite communication for small satellite systems: Physical layer to network layer view," *IEEE Commun. Surveys Tuts.*, vol. 18, no. 4, pp. 2442–2473, 4th Quart., 2016.
[9] A. Golkar and I. Lluch i Cruz, "The federated satellite systems paradigm: Concept and business case evaluation," *Acta Astronautica*, vol. 111, pp. 230–248, Jun. 2015.
[10] J. A. Ruiz de Azua, A. Calveras, and A. Camps, "Internet of satellites (IoSat): Analysis of network models and routing protocol requirements," *IEEE Access*, vol. 6, pp. 20390–20411, 2018.
[11] J. A. Ruiz-De-Azua, A. Camps, and A. C. Auge, "Benefits of using mobile ad-hoc network protocols in federated satellite systems for polar satellite missions," *IEEE Access*, vol. 6, pp. 56356–56367, 2018.
[12] A. Ehsanfar and P. T. Grogan, "Auction-based algorithms for routing and task scheduling in federated networks," *J. Netw. Syst. Manage.*, vol. 28, no. 2, pp. 271–297, Apr. 2020.
[13] A. Ehsanfar and P. T. Grogan, "Mechanism design for exchanging resources in federated networks," *J. Netw. Syst. Manage.*, vol. 28, no. 1, pp. 108–132, Jan. 2020.
[14] U. Pica and A. Golkar, "Sealed-bid reverse auction pricing mechanisms for federated satellite systems," *Syst. Eng.*, vol. 20, no. 5, pp. 432–446, Sep. 2017.
[15] I. Lluch, P. T. Grogan, U. Pica, and A. Golkar, "Simulating a proactive ad-hoc network protocol for federated satellite systems," in *Proc. IEEE Aerosp. Conf.*, Mar. 2015, pp. 1–16.
[16] J. A. Ruiz-de-Azua, A. Calveras, A. Golkar, A. Camps, L. Fernandez, J. F. Munoz, M. Badia, R. Castella, C. Diez, A. Aguilella, S. Briatore, and N. Garzaniti, "Proof-of-concept of a federated satellite system between two 6-Unit CubeSats for distributed Earth observation satellite systems," in *Proc. IEEE Int. Geosci. Remote Sens. Symp. IGARSS*, Jul. 2019, pp. 8871–8874.
[17] I. del Portillo, B. G. Cameron, and E. F. Crawley, "A technical comparison of three low Earth orbit satellite constellation systems to provide global broadband," *Acta Astronautica*, vol. 159, pp. 123–135, Jun. 2019.
[18] J. A. Ruiz-de-Azua, C. Araguz, A. Calveras, E. Alarcon, and A. Camps, "Towards an integral model-based simulator for autonomous Earth observation satellite networks," in *Proc. IEEE Int. Geosci. Remote Sens. Symp. IGARSS*, Jul. 2018, pp. 7403–7406.
[19] A. R. Carrel and P. L. Palmer, "An evolutionary algorithm for near-optimal autonomous resource management," in *Proc. 8th Int. Symp. Artif. Intell., Robot. Automat. Space*, Sep. 2005, pp. 1–8.
[20] C. Araguz, E. Bou-Balust, and E. Alarcón, "Applying autonomy to distributed satellite systems: Trends, challenges, and future prospects," *Syst. Eng.*, vol. 21, no. 5, pp. 401–416, Sep. 2018.
[21] S. Chien, M. Johnston, J. Frank, M. Giuliano, A. Kavelaars, C. Lenzen, and N. Policella, "A generalized timeline representation, services, and interface for automating space mission operations," in *Proc. SpaceOps Conf.*, Jun. 2012, Art. no. 1275459.
[22] M. Geyer, F. Mrowka, and C. Lenzen, "Terrasar-x/tandem-x mission planning-handling satellites in close formation," in *Proc. SpaceOps Conf. Delivering Dream Hosted NASA Marshall Space Flight Center Organized AIAA*, 2010, p. 1989.
[23] A. Neumann, C. Aichele, M. Lindner, and S. Wunderlich, "Better approach to mobile ad-hoc networking (batman)," IETF Draft, Apr. 2008, pp. 1–24.
[24] A. Neumann, E. Lopez, and L. Navarro, "An evaluation of BMX6 for community wireless networks," in *Proc. IEEE 8th Int. Conf. Wireless Mobile Comput., Netw. Commun. (WiMob)*, Oct. 2012, pp. 651–658.
[25] I. Lluch and A. Golkar, "Design implications for missions participating in federated satellite systems," *J. Spacecraft Rockets*, vol. 52, no. 5, pp. 1361–1374, Sep. 2015.
[26] World Meteorological Organization. (2011). *Observing Systems Capability Analysis and Review Tool*. Accessed: Apr. 22, 2020. [Online]. Available: https://www.wmo-sat.info/oscar/spacecapabilities
[27] Kelso, Thomas Sean. (1985). *Celestrak*. Accessed: Apr. 22, 2020. [Online]. Available: https://celestrak.com
[28] Gomspace Aps. (2018). *Nanocom sr2000*. Accessed: Apr. 21, 2020. [Online]. Available: https://gomspace.com/UserFiles/Subsystems/datasheet/gs-ds-nanocom-sr200%0-20.pdf
[29] Tyvak Nano-Satellite Systems, Inc. (2019). *Platforms*. Accessed: Apr. 21, 2020. [Online]. Available: https://www.tyvak.com/mp-files/tyvak_platforms.pdf
[30] United States Geological Survey (USGS). *Landsat Missions—Landsat 8*. Accessed: May 12, 2020. [Online]. Available: https://www.usgs.gov/land-resources/nli/landsat/landsat-8?qt-science_su%pport_page_related_con=0#qt-science_support_page_related_con
[31] eoPortal Directory. *Terrasar-x Mission*. Accessed: May 12, 2020. [Online]. Available: https://earth.esa.int/web/eoportal/satellite-missions/t/terrasar-x
[32] D. Barbaric, J. Vukovic, and D. Babic, "Link budget analysis for a proposed cubesat Earth observation mission," in *Proc. 41st Int. Conv. Inf. Commun. Technol., Electron. Microelectron. (MIPRO)*, May 2018, pp. 0133–0138.
[33] S. R. Pratt, R. A. Raines, C. E. Fossa, and M. A. Temple, "An operational and performance overview of the IRIDIUM low Earth orbit satellite system," *IEEE Commun. Surveys Tuts.*, vol. 2, no. 2, pp. 2–10, 2nd Quart., 1999.

[34] L. Léon, P. Koch, and R. Walker, "Gomx-4-the twin European mission for IOD purposes," in *Proc. 32nd Annu. AIAA/USU Conf. Small Satell.*, 2018, pp. 4–9.
[35] S. Briatore, R. Akhtyamov, and A. Golkar, "Design and flight test results of high speed optical bidirectional link between stratospheric platforms for aerospace applications," *Proc. SPIE*, vol. 10408, Aug. 2017, Art. no. 1040804.
[36] V. Yazıcı, U. Kozat, and M. Sunay, "A new control plane for 5G network architecture with a case study on unified handoff, mobility, and routing management," *IEEE Commun. Mag.*, vol. 52, no. 11, pp. 76–85, Nov. 2014.
[37] S. C. W. Sensing and T. P. Division, "An1200.22: Lora^{T}M modulation basics," Semtech Corp., Camarillo, CA, USA, Tech. Rep. AN1200.22, 2015. [Online]. Available: http://wiki.lahoud.fr/lib/exe/fetch.php?media=an1200.22.pdf
[38] U. Raza, P. Kulkarni, and M. Sooriyabandara, "Low power wide area networks: An overview," *IEEE Commun. Surveys Tuts.*, vol. 19, no. 2, pp. 855–873, 2nd Quart., 2017.
[39] R. Ratasuk, N. Mangalvedhe, Y. Zhang, M. Robert, and J.-P. Koskinen, "Overview of narrowband IoT in LTE rel-13," in *Proc. IEEE Conf. Standards for Commun. Netw. (CSCN)*, Oct. 2016, pp. 1–7.
[40] 3rd Generation Partnership Project. (2020). *3GPP: The Mobile Broadband Standard*. Accessed: Apr. 22, 2020. [Online]. Available: https://www.3gpp.org/
[41] L. Vangelista, A. Zanella, and M. Zorzi, "Long-range IoT technologies: The dawn of LoRa," in *Future Access Enablers of Ubiquitous and Intelligent Infrastructures*. Springer, 2015, pp. 51–58.
[42] H. Caleb. (2019). *Lacuna Space Aims to Ride IoT Wave With a 32-Cubesat Constellation*. Accessed: Apr. 22, 2020. [Online]. Available: https://spacenews.com/lacuna-space-aims-to-ride-iot-wave-with-a-32-cube%sat-constellation/
[43] A. A. Doroshkin, A. M. Zadorozhny, O. N. Kus, V. Y. Prokopyev, and Y. M. Prokopyev, "Experimental study of LoRa modulation immunity to Doppler effect in CubeSat radio communications," *IEEE Access*, vol. 7, pp. 75721–75731, 2019.
[44] L. Fernandez, J. A. Ruiz-de-Azua, A. Calveras, and A. Camps, "Evaluation of LoRa for data retrieval of ocean monitoring sensors with LEO satellites," in *Proc. IEEE Int. Geosci. Remote Sens. Symp. (IGARSS)*, Sep. 2020.
[45] F. Systems. (2020). *Fossasat-1*. Accessed: May 12, 2020. [Online]. Available: https://fossa.systems/
[46] *LLC: Spacex Ka-Band NGSO Constellation FCC Filing SAT-LOA-20161115-00118*, Holdings Space Explor., Washington, DC, USA, 2018.
[47] A. Sayin, M. Cherniakov, and M. Antoniou, "Passive radar using starlink transmissions: A theoretical study," in *Proc. 20th Int. Radar Symp. (IRS)*, Jun. 2019, pp. 1–7.
[48] J. A. Ruiz-de-Azua, V. Ramírez, H. Park, A. Calveras, and A. Camps, "Predictive algorithms to assess inter-satellite links availability in autonomous satellite networks," in *International Astronautical Congress (IAC)*. New Delhi, India, IAF, 2019.
[49] C. Araguz, J. A. Ruiz-de-Azua, A. Calveras, A. Camps, and E. Alarcon, "Simulating distributed small satellite networks: A model-based tool tailored to decentralized resource-constrained systems," in *Proc. 70th Int. Astron. Congr. (IAC)*. New Delhi, India, IAF, 2019, pp. 1–10.
[50] nsnam. (2020). *Ns-3: Network Simulator*. Accessed: May 21, 2020. [Online]. Available: https://www.nsnam.org
[51] E. W. Dijkstra, "A note on two problems in connexion with graphs," *Numerische Math.*, vol. 1, no. 1, pp. 269–271, Dec. 1959.
[52] C. Vinton, S. Burleigh, A. Hooke, L. Torgerson, R. Durst, K. Scott, K. Fall, and H. Weiss, *Delay-Tolerant Networking Architecture*. document RFC 4838, RFC Editor, 2007.
[53] G. Araniti, N. Bezirgiannidis, E. Birrane, I. Bisio, S. Burleigh, C. Caini, M. Feldmann, M. Marchese, J. Segui, and K. Suzuki, "Contact graph routing in DTN space networks: Overview, enhancements and performance," *IEEE Commun. Mag.*, vol. 53, no. 3, pp. 38–46, Mar. 2015.
[54] B. Book, "Schedule-aware bundle routing," in *Consultative Committee for Space Data Systems (CCSDS)*. Washington, DC, USA: CCSDS Secretariat, Jul. 2019.
[55] J. A. Fraire and J. M. Finochietto, "Design challenges in contact plans for disruption-tolerant satellite networks," *IEEE Commun. Mag.*, vol. 53, no. 5, pp. 163–169, May 2015.
[56] M. Marchese and F. Patrone, "E-CGR: Energy-aware contact graph routing over nanosatellite networks," *IEEE Trans. Green Commun. Netw.*, early access, Mar. 20, 2020, doi: 10.1109/TGCN.2020.2978296.
[57] D. Zhou, M. Sheng, X. Wang, C. Xu, R. Liu, and J. Li, "Mission aware contact plan design in resource-limited small satellite networks," *IEEE Trans. Commun.*, vol. 65, no. 6, pp. 2451–2466, Jun. 2017.
[58] J. A. Ruiz-De-Azua, V. Ramirez, H. Park, A. C. Auge, and A. Camps, "Assessment of satellite contacts using predictive algorithms for autonomous satellite networks," *IEEE Access*, vol. 8, pp. 100732–100748, 2020.
[59] M. Werner, C. Delucchi, H.-J. Vogel, G. Maral, and J.-J. De Ridder, "ATM-based routing in LEO/MEO satellite networks with intersatellite links," *IEEE J. Sel. Areas Commun.*, vol. 15, no. 1, pp. 69–82, Jan. 1997.

JOAN A. RUIZ-DE-AZUA (Member, IEEE) was born in Barcelona, Spain. He received the degrees in aerospace engineering from Supaero, Toulouse, France, and the Telecommunications Engineering degree from the Unversitat Politècnica de Catalunya, Barcelona, in 2015, and the M.S. degree in network protocols from Supaero, in 2015. He is currently pursuing the Ph.D. degree with the Universitat Politècnica de Catalunya. He has participated in different projects of ground segment for Ariane 5 and Ariane 6 in GTD company. He is currently participating in the Fly Your Satellite Program of the ESA. He is a member of the FSSCat project, which is the winner of the ESA Sentinel Small Sat (S^3) Challenge of the Copernicus Masters Competition. His research interests include satellite architectures, satellite networks, the Internet of Things, and embedded software. He received the Best M.S. Thesis Award on Critical Communications from the Official Spanish Telecommunications Chartered Institute, in 2016.

ANNA CALVERAS was born in Barcelona, Spain, in 1969. She received the Ph.D. degree in telecommunications engineering from the Universitat Politècnica de Catalunya, Spain, in 2000. She is currently an Associate Professor at the Computer Networks Department, Wireless Networks Group (WNG), Universitat Politècnica de Catalunya. She has been involved in several national and international research or technology transfer projects. She has published in international and national conferences and journals. Her research interests include the design, evaluation, and optimization of communications protocols and architectures for cellular, wireless multihop networks, ad hoc networks, wireless sensor networks, the Internet of Things, and application domains, such as smart cities, building automation, and emergency environments.

ADRIANO CAMPS (Fellow, IEEE) was born in Barcelona, Spain, in 1969. He received the degree in telecommunications engineering and the Ph.D. degree in telecommunications engineering from the Universitat Politècnica de Catalunya (UPC), Barcelona, in 1992 and 1996, respectively. From 1991 to 1992, he was at the ENS des Télécommunications de Bretagne, France, with an Erasmus Fellowship. Since 1993, he has been with the Electromagnetics and Photonics Engineering Group, Department of Signal Theory and Communications, UPC, where he was an Assistant Professor and an Associate Professor, in 1997, and has been a Full Professor, since 2007. He has published more than 210 journal articles in peer-reviewed journals and more than 425 international conference presentations and holds 12 patents. His research interests include microwave remote sensing, with a special emphasis on microwave interferometric radiometry by aperture synthesis (ESA's SMOS mission), passive microwave remote sensing using signals of opportunity (GNSS-Reflectometry), and the use of nano-satellites as cost-effective platforms to test innovative concepts for earth observation, such as the 3Cat-2, a 6U-class cubesat mission launched, in August 2016, carrying onboard an innovative GNSS-R payload.